^{3}He Spin-Dependent Cross Sections and Sum Rules

K. Slifer,[29†] M. Amarian,[34] L. Auerbach,[29] T. Averett,[10,33] J. Berthot,[4] P. Bertin,[4] B. Bertozzi,[18] T. Black,[18] E. Brash,[24] D. Brown,[17] E. Burtin,[27] J. Calarco,[20] G. Cates,[23,32] Z. Chai,[18] J.-P. Chen,[10] Seonho Choi,[29] E. Chudakov,[10] C. Ciofi degli Atti,[6,22] E. Cisbani,[8] C.W. de Jager,[10] A. Deur,[4,10,32] R. DiSalvo,[4] S. Dieterich,[26] P. Djawotho,[33] M. Finn,[33] K. Fissum,[18] H. Fonvieille,[4] S. Frullani,[8] H. Gao,[18,31] J. Gao,[1] F. Garibaldi,[8] A. Gasparian,[3] S. Gilad,[18] R. Gilman,[10,26] A. Glamazdin,[14] C. Glashausser,[26] W. Glöckle,[5] J. Golak,[16] E. Goldberg,[1] J. Gomez,[10] V. Gorbenko,[14] J.-O. Hansen,[10] B. Hersman,[20] R. Holmes,[28] G.M. Huber,[24] E. Hughes,[1] B. Humensky,[23] S. Incerti,[29] M. Iodice,[8] S. Jensen,[1] X. Jiang,[26] C. Jones,[1] G. Jones,[12] M. Jones,[33] C. Jutier,[4,21] H. Kamada,[15] A. Ketikyan,[34] I. Kominis,[23] W. Korsch,[12] K. Kramer,[33] K. Kumar,[19,23] G. Kumbartzki,[26] M. Kuss,[10] E. Lakuriqi,[29] G. Laveissiere,[4] J. J. Lerose,[10] M. Liang,[10] N. Liyanage,[10,18] G. Lolos,[24] S. Malov,[26] J. Marroncle,[27] K. McCormick,[21] R. D. McKeown,[1] Z.-E. Meziani,[29] R. Michaels,[10] J. Mitchell,[10] A. Nogga,[13] E. Pace,[9,25] Z. Papandreou,[24] T. Pavlin,[1] G.G. Petratos,[11] D. Pripstein,[1] D. Prout,[11] R. Ransome,[26] Y. Roblin,[4] D. Rowntree,[18] M. Rvachev,[18] F. Sabatié,[21,27] A. Saha,[10] G. Salmè,[7] S. Scopetta,[6,22] R. Skibiński,[16] P. Souder,[28] T. Saito,[30] S. Strauch,[26] R. Suleiman,[11] K. Takahashi,[30] S. Teijiro,[30] L. Todor,[21] H. Tsubota,[30] H. Ueno,[30] G. Urciuoli,[8] R. Van der Meer,[10,24] P. Vernin,[27] H. Voskanian,[34] H. Witała,[16] B. Wojtsekhowski,[10] F. Xiong,[18] W. Xu,[18] J.-C. Yang,[2] B. Zhang,[18] P. Zolnierczuk[12]

(Jefferson Lab E94010 Collaboration)

[1] *California Institute of Technology, Pasadena, California 91125*
[2] *Chungnam National University, Taejon 305-764, Korea*
[3] *Hampton University, Hampton, Virginia 23668*
[4] *LPC IN2P3/CNRS, Université Blaise Pascal, F–63170 Aubière Cedex, France*
[5] *Institut für Theoretische Physik II,Ruhr Universität Bochum, D-44780 Bochum, Germany*
[6] *INFN, Sezione di Perugia, 06100, Perugia, Italy*
[7] *INFN, Sezione Roma I, P.le A. Moro 2, I-00185, Roma, Italy.*
[8] *INFN, Sezione Sanità, 00161 Roma, Italy*
[9] *INFN, Sezione Tor Vergata, via della Ricerca Scientifica 1, I 00133 Roma, Italy.*
[10] *Thomas Jefferson National Accelerator Facility, Newport News, Virginia 23606*
[11] *Kent State University, Kent, Ohio 44242*
[12] *University of Kentucky, Lexington, Kentucky 40506*
[13] *Institut für Kernphysik, Forschungszentrum Jülich, 52425 Jülich, Germany*
[14] *Kharkov Institute of Physics and Technology, Kharkov 310108, Ukraine*

[†] Presently at University of Virginia

[15] *Department of Physics, Faculty of Engineering, Kyushu Institute of Technology, 1-1 Sensuicho, Tobata, Kitakyushu 804-8550, Japan*
[16] *M. Smoluchowski Institute of Physics, Jagiellonian University, PL-30059 Krakòw, Poland*
[17] *University of Maryland, College Park, Maryland 20742*
[18] *Massachusetts Institute of Technology, Cambridge, Massachusetts 02139*
[19] *University of Massachusetts-Amherst, Amherst, Massachusetts 01003*
[20] *University of New Hampshire, Durham, New Hamphsire 03824*
[21] *Old Dominion University, Norfolk, Virginia 23529*
[22] *Dipartimento di Fisica, Perugia University*
[23] *Princeton University, Princeton, New Jersey 08544*
[24] *University of Regina, Regina, SK S4S 0A2, Canada*
[25] *Dipartimento di Fisica, Universita' di Roma "Tor Vergata", Rome, Italy*
[26] *Rutgers, The State University of New Jersey, Piscataway, New Jersey 08855*
[27] *CEA Saclay, IRFU/SPhN, 91191 Gif/Yvette, France*
[28] *Syracuse University, Syracuse, New York 13244*
[29] *Temple University, Philadelphia, Pennsylvania 19122*
[30] *Tohoku University, Sendai 980, Japan*
[31] *Triangle Universities Nuclear Laboratory, Duke Univ. Durham, NC 27708.*
[32] *University of Virginia, Charlottesville, Virginia 22904*
[33] *The College of William and Mary, Williamsburg, Virginia 23187*
[34] *Yerevan Physics Institute, Yerevan 375036, Armenia*

(Dated: March 19, 2008)

Abstract

We present a measurement of the spin-dependent cross sections for the $^3\vec{\mathrm{H}}\mathrm{e}(\vec{\mathrm{e}},\mathrm{e}')\mathrm{X}$ reaction in the quasielastic and resonance regions at four-momentum transfer $0.1 \leq Q^2 \leq 0.9$ GeV^2. The spin-structure functions have been extracted and used to evaluate the nuclear Burkhardt–Cottingham and extended GDH sum rules for the first time. Impulse approximation and exact three-body Faddeev calculations are also compared to the data in the quasielastic region.

PACS numbers: 11.55.Hx,11.55.Fv,25.30.Rw,12.38.Qk,13.60.Hb,29.25.Pj,29.27.Hj,25.70.Bc

Inclusive electron scattering has been used extensively to investigate the fundamental gauge theory of the strong interaction, quantum chromodynamics (QCD). One goal of this endeavor has been a greater understanding of the spin-structure of the nucleon. The wealth of experimental data (e.g. [1, 2]), collected in recent years is crucial for testing the implementations of QCD: the operator product expansion (OPE) at large four-momentum transfer Q^2, chiral perturbation theory (χPT) at low Q^2, and lattice gauge theory in the intermediate region. χPT, in particular, has had success in describing polarized nucleon data [3], but has also met with some interesting challenges [4, 5].

The spin-dependent contributions to the inclusive cross section of a spin-1/2 system are contained in the structure functions g_1 and g_2, or equivalently the cross sections σ'_{TT} and σ'_{LT}. Spin-dependent measurements in the simplest systems have been the focus of several recent investigations [6, 7, 8, 9] at low to moderate Q^2. Fundamental sum rules govern the behavior of the nucleon spin-structure functions, but the assumptions made in deriving these relations apply regardless of whether the target is a nucleon or a nucleus. For example, the Gerasimov-Drell-Hearn (GDH) sum rule [10] was derived for a nucleon target, but is also valid for nuclei. For a target of spin $\mathcal{S}$, mass M, and anomalous magnetic moment κ, it reads:

$$\int_{\nu_{\mathtt{th}}}^{\infty} \frac{\sigma_{\mathtt{A}}(\nu) - \sigma_{\mathtt{P}}(\nu)}{\nu} d\nu = -4\pi^2 \mathcal{S} \alpha \left(\frac{\kappa}{M}\right)^2 \tag{1}$$

Here $\sigma_{\mathtt{A}}(\sigma_{\mathtt{P}})$ represents the cross section for absorption of a photon of energy ν which is polarized anti-parallel (parallel) to the target spin and α is the fine-structure constant. The inelastic threshold is signified by $\nu_{\mathtt{th}}$, which is pion production (photodisintegration) for a nucleonic (nuclear) target. Due to the $1/\nu$-weighting, states with lower invariant mass provide the most significant contribution to the sum rule. The GDH predictions for the neutron and ^{3}He are -234 and -496 μb, respectively. To gauge the relative strength of the nuclear contribution [11] to Eq. 1, we divide the ^{3}He integral into two excitation energy regions. Region I extends from two-body breakup to the pion production threshold, and region II extends from threshold to ∞. Polarized ^{3}He at first order appears as a free polarized neutron due to the spin pairing of the protons, so the contribution from region II should be approximately -234 μb. Therefore, the contribution in region I is necessarily quite large in order to satisfy the prediction for ^{3}He. The only reaction available to real photons in region I is disintegration, and Arenhövel [11] points out that threshold disintegration must

become significant at low Q^2 in order to satisfy the sum rule prediction for the lightest nuclear systems.

Ji and Osborne [12] suggest a generalization of the GDH sum rule based on the relationship between the forward virtual Compton amplitudes S_1 and S_2, and the spin-dependent structure functions. Since Eq. 1 is derived from the dispersion relation for S_1 at the real photon point, a generalized sum rule can also be constructed from the same relation at nonzero Q^2. This leads to a set of Q^2-dependent dispersion relations [13] for the spin-structure functions. In particular, the dispersion relation for S_1 leads to the following extension of the GDH sum rule to virtual-photon scattering:

$$\overline{\Gamma}_1(Q^2) \equiv \int_0^{1-\epsilon} g_1(x,Q^2)dx = \frac{Q^2}{8}\,\overline{S}_1(0,Q^2) \tag{2}$$

The infinitesimal ϵ insures that only inelastic contributions are included, which is indicated by the overbar, and $x = Q^2/2M\nu$ is the Bjorken scaling variable. However, an alternate extension is often presented [14]:

$$\begin{aligned} I(Q^2) &= \int_{\nu_{th}}^{\infty} \frac{\sigma_A(\nu,Q^2) - \sigma_P(\nu,Q^2)}{\nu} d\nu \\ &= 2\int_{\nu_{th}}^{\infty} \frac{K}{\nu}\frac{\sigma_{TT'}(\nu,Q^2)}{\nu} d\nu \end{aligned} \tag{3}$$

Here, K is the virtual photon flux factor, and $\sigma_{TT'}$ is the transverse-transverse cross section for scattering with target spin aligned along the direction of the three-momentum transfer $\vec{q}$. We will also refer to $\sigma_{LT'}$, the longitudinal-transverse cross section for scattering with target spin perpendicular to the momentum transfer.

The dispersion relation for S_2 leads [13] to the following super-convergence relation:

$$\Gamma_2(Q^2) \equiv \int_0^1 g_2(x,Q^2)dx = 0 \tag{4}$$

which is the Burkhardt–Cottingham (BC) sum rule [15]. The derivation of the BC sum rule depends on the convergence of the integral, and assumes that g_2 is a well-behaved function [16] as $x \to 0$. It has been shown to be satisfied at first order in α_s for a quark target in pQCD [17], and to lowest order in α_{em} in QED [18].

This Letter details a test of the sum rules described above via an inclusive cross-section measurement in the quasielastic (QE) and resonance regions. The experiment was performed in Hall A [19] of the Thomas Jefferson National Accelerator Facility (JLab). Longitudinally

polarized electrons at six incident energies from 0.9 to 5.1 GeV were scattered from a high-density polarized ^{3}He target. Longitudinal and transverse target polarizations were maintained, allowing a precision determination of both $g_1^{^3\mathrm{He}}(x,Q^2)$ and $g_2^{^3\mathrm{He}}(x,Q^2)$ or alternatively $\sigma_{TT'}(\nu,Q^2)$ and $\sigma_{LT'}(\nu,Q^2)$. Full experimental details can be found in Refs. [4, 8, 9]

The measured spin-structure functions were interpolated (or extrapolated for a few data points at large ν) to constant Q^2 [8] from 0.1 to 0.9 GeV^2. Figure 1 displays the first moments of $g_1^{^3\mathrm{He}}$ and $g_2^{^3\mathrm{He}}$, along with the extended GDH sum $I(Q^2)$. In all panels the circles represent the ^{3}He data integrated to $W = 2$ GeV. The invariant mass W is defined here in terms of the proton mass: $W^2 = M_p^2 - Q^2 + 2M_p\nu$. Squares include an estimate (discussed below) of any unmeasured contributions. Statistical uncertainties are shown on the data points, while the systematic uncertainty of the measured (total) integral is represented by the light (dark) band. The absolute cross sections contribute 5% uncertainty, while the beam and target polarization each contribute 4%. The radiative corrections are assigned 20% uncertainty to reflect the variation seen from choosing different initial models for our unfolding procedure. This uncertainty is doubled for the 0.9 GeV incident energy spectra to reflect the lack of lower energy data. A separate contribution to the radiative corrections uncertainty arises from the subtraction of the ^{3}He elastic radiative tail, which is significant only for the lowest incident energy. The uncertainty due to interpolation has been determined by varying the order of the polynomial interpolation, while the extrapolation uncertainty has been estimated by comparison to model [20] predictions. The light band represents the quadratic sum of the above errors. The full systematic band includes an estimate of the uncertainty of the unmeasured contribution to the integrals. The Γ_2 full systematic error includes a 5% uncertainty from the elastic contribution (solid black curve) which was evaluated using previously measured form factors [21].

The total integral of $\overline{\Gamma}_1$ includes an estimate [22] of the unmeasured region above $W = 2$ GeV, and the uncertainty arising from this is reflected in the total error band. The data show some hint of a turnover at low Q^2, where we have also plotted the slope predicted by Eq. 1 for ^{3}He. To obtain the model curve, we have summed the MAID [20] proton and neutron predictions using an effective polarization procedure [23]. To this we add an estimate of the contribution below the pion threshold using the plane-wave impulse approximation (PWIA) model [24, 25]. At large momentum transfer, $\Gamma_1(Q^2)$ appears to be nearly independent of Q^2. This is consistent with an OPE interpretation in which the higher twist effects become

negligible at large Q^2 and the evolution is driven by logarithmic pQCD effects. It is somewhat surprising to observe this behavior in a region where the higher twists are conventionally expected to be quite significant. However, this is consistent with other recent findings (eg. [26, 27]) in this kinematic range.

Experimental measurements of g_2 are scarce and only recently has the BC sum rule been evaluated for the first time. The SLAC E155 collaboration [28] measured Γ_2 at $Q^2 = 5$ GeV^2. They found the BC sum rule to be satisfied within a large uncertainty for the deuteron, while a violation of almost 3σ was found for the more precise proton measurement. In Figure 1 (middle) we plot Γ_2. The unmeasured contribution was estimated using the method described in [28], which assumes the validity of the Wandzura-Wilczek relation [29]. All six data points are consistent with the Burkhardt–Cottingham prediction. Results from this same experiment have been used to test the BC sum rule for the neutron [9], using only data for which $W > 1.073$ GeV, and with nuclear corrections applied. It was found that the neutron BC sum rule is satisfied primarily due to the cancellation of the resonance and nucleon elastic contributions. It is interesting to find that for ^{3}He a balance is struck between the positive inelastic contribution above the pion threshold, and the negative contribution from the elastic and quasielastic regions, with the elastic becoming important below $Q^2 \approx 0.2$ GeV^2.

Figure 1 (bottom) displays the extended GDH sum as defined in Eq. 3. We follow the convention $K = \nu$ for the virtual photon flux. Accounting for the unmeasured contribution [22] has only a minor effect due to the $1/\nu$-weighting of the integrand. The phenomenological model (dot-dashed curve) tracks the data well, but the negative sum rule prediction at $Q^2 = 0$ (black star) stands in contrast to the large positive value of our lowest point. The ^{3}He GDH integral is dominated by a positive QE contribution which largely outweighs the negative contribution of the resonances. Assuming the continuity of the integrand as $Q^2 \to 0$, as in the nucleonic case [30], our results indicate the necessity of a dramatic turnover in $I(Q^2)$ at very low Q^2. The only possible reaction channel available to accommodate such a turnover is electro-disintegration at threshold. Indeed, our σ'_{TT} data [31] shows an indication of a growing negative contribution to the sum in the threshold region as Q^2 approaches zero. A recently completed experiment [32] in the range $0.02 < Q^2 < 0.3$ GeV^2 may shed further light on this behavior.

We focus now on the quasielastic region, where ^{3}He can be treated with exact nonrela-

tivistic Faddeev calculations. This approach describes the existing data [33, 34, 35] well at low Q^2. At larger Q^2, modern applications [24, 25] of the PWIA have had good success reproducing data. The measured quasielastic differential cross section $d\sigma/d\Omega dE'$ is displayed in Figure 2 as a function of W. In addition, Figure 3 displays the ^{3}He polarized cross sections $\sigma_{TT'}$ and $\sigma_{LT'}$. Radiative corrections have been applied to the data as discussed in Refs. [8, 31]. The data are compared to a PWIA calculation [24, 25] and an exact nonrelativistic Faddeev calculation [34, 35, 36]. The latter includes both final state interactions (FSI) and meson exchange currents (MEC). Both groups utilize the Höhler [37] parameterization for the single nucleon current, and the AV18 [38] nucleon-nucleon potential. We also display the PWIA curves that result when the RSC [24, 25] potential is used instead of AV18, or if the Galster [39] form factor parameterization is used instead of Höhler. In the Faddeev calculation, the three-nucleon current operator consists of the single nucleon current and the π- and ρ-like meson exchange contributions consistent with AV18.

The Faddeev calculation does not address relativistic effects, and as such was only performed for the lowest Q^2 data. The agreement with data is in general quite good, but we find a small discrepancy from the data on the high energy side of the QE peak at $\langle Q^2 \rangle = 0.2$ GeV^2. This may indicate the increasing importance of relativistic effects, along with the growth in relative strength of the Δ resonance tail in the QE region as Q^2 increases. We note that $\sigma_{LT'}$ which is not sensitive to the Δ resonance generally shows better agreement with the Faddeev calculation on the high energy side of the quasielastic peak.

At very low Q^2, the PWIA calculation fails, but improves as expected with increasing momentum transfer, in part because it takes the relativistic kinematics into account. The fact that the Faddeev and PWIA calculations differ less as Q^2 increases seems to indicate that FSI and MEC (neglected in the PWIA) become less important for these observables as Q^2 increases. It also appears that the PWIA calculation is more sensitive to the choice of the form factor parameterization, than to the nucleon-nucleon potential utilized.

The Faddeev calculation reproduces the polarized data well at the lowest Q^2, and the PWIA does well at the highest, but there remains an intermediate zone where both approaches are unsatisfactory. Refs. [34, 35] previously reported that this same PWIA calculation reproduced well the measured ^{3}He quasielastic asymmetry A'_T in this kinematic region. As such we compared this calculation directly to the transverse asymmetry A'_T data from our experiment and found good agreement, consistent with the previous results but only in

a narrow window centered on the QE peak.

To summarize, we find the Burkhardt–Cottingham sum rule to hold for ^{3}He. The GDH integral and Γ_1 display intriguing behavior at low Q^2, and will provide valuable constraints on future ^{3}He χPT and lattice QCD calculations. We have measured the first precision polarized cross-sections in the quasielastic and resonance regions of ^{3}He. A full three-body Faddeev calculation agrees well with the data, but starts to exhibit discrepancies as the energy increases, possibly due to growing relativistic effects. As the momentum transfer increases, the PWIA approach reproduces the data well, but there exists an intermediate range where neither calculation succeeds.

This work was supported by the U.S. Department of Energy, the National Science Foundation, the French Commissariat à l'Energie Atomique (CEA), the Centre National de la Recherche Scientifique (CNRS) and by the Helmholtz Association through the virtual institute "Spin and strong QCD" (VH-VI-231). The numerical calculations were performed on the IBM Regatta p690+ of the NIC in Jülich, Germany. The Southeastern Universities Research Association operates the Thomas Jefferson National Accelerator Facility for the DOE under contract DE-AC05-84ER40150, mod. # 175.

[1] B. W. Filippone and X.-D. Ji, Adv. Nucl. Phys. **26**, 1 (2001).

[2] J. P. Chen, A. Deur, and Z.-E. Meziani, Mod. Phys. Lett. **A20**, 2745 (2005).

[3] V. Bernard, Prog. Part. Nucl. Phys. **60**, 82 (2008).

[4] M. Amarian et al., Phys. Rev. Lett. **93**, 152301 (2004).

[5] Y. Prok et al. (2008), arXiv:0802.2232 [nucl-ex].

[6] P. E. Bosted et al., Phys. Rev. **C75**, 035203 (2007).

[7] K. Dharmawardane et al., Phys. Lett. **B641**, 11 (2006).

[8] M. Amarian et al., Phys. Rev. Lett. **89**, 242301 (2002).

[9] M. Amarian et al., Phys. Rev. Lett. **92**, 022301 (2004).

[10] S. Gerasimov, Sov. J. Nucl. Phys. **2**, 430 (1966); S. D. Drell and A. C. Hearn , Phys. Rev. Lett. **16**, 908 (1966); M. Hosoda and K. Yamamoto, Prog. Theor. Phys. **30**, 425 (1966).

[11] H. Arenhövel, Proceedings, GDH2000, pg. 67. World Scientific. nucl-th/0006083.

[12] X. Ji and J. Osborne, J. Phys. **G27**, 127 (2001).

[13] D. Drechsel, B. Pasquini, and M. Vanderhaeghen, Phys. Rept. **378**, 99 (2003).

[14] D. Drechsel, S. S. Kamalov, and L. Tiator, Phys. Rev. **D63**, 114010 (2001).

[15] H. Burkhardt and W. N. Cottingham, Annals Phys. **56**, 453 (1970).

[16] R. L. Jaffe and X.-D. Ji, Phys. Rev. **D43**, 724 (1991).

[17] G. Altarelli, B. Lampe, P. Nason, and G. Ridolfi, Phys. Lett. **B334**, 187 (1994).

[18] W.-Y. Tsai, L. L. DeRaad Jr., and K. A. Milton, Phys. Rev. **D11**, 3537 (1975).

[19] J. Alcorn et al., Nucl. Instrum. Meth. **A522**, 294 (2004).

[20] D. Drechsel, O. Hanstein, S. S. Kamalov, and L. Tiator, Nucl. Phys. **A645**, 145 (1999).

[21] A. Amroun et al., Nucl. Phys. **A579**, 596 (1994).

[22] E. Thomas and N. Bianchi, Nucl. Phys. Proc. Suppl. **82**, 256 (2000).

[23] C. Ciofi degli Atti and S. Scopetta, Phys. Lett. **B404**, 223 (1997).

[24] C. Ciofi degli Atti, E. Pace, and G. Salme, Phys. Rev. **C51**, 1108 (1995).

[25] E. Pace, G. Salme, S. Scopetta, and A. Kievsky, Phys. Rev. **C64**, 055203 (2001).

[26] Z.-E. Meziani et al., Phys. Lett. **B613**, 148 (2005).

[27] A. Deur et al., Phys. Rev. Lett. **93**, 212001 (2004).

[28] P. L. Anthony et al. (E155), Phys. Lett. **B553**, 18 (2003).

[29] S. Wandzura and F. Wilczek, Phys. Lett. **B72**, 195 (1977).

[30] H. Arenhövel, D. Drechsel, and H. J. Weber, Nucl. Phys. **A305**, 485 (1978).

[31] K. Slifer, Ph.D. thesis, Temple University (2004).

[32] J.-P. Chen, A. Deur, and F. Garibaldi, spokespersons JLab Experiment E97110.

[33] C. M. Spaltro et al., Phys. Rev. Lett. **81**, 2870 (1998).

[34] W. Xu et al., Phys. Rev. Lett. **85**, 2900 (2000).

[35] F. Xiong et al., Phys. Rev. Lett. **87**, 242501 (2001).

[36] J. Golak et al., Phys. Rept. **415**, 89 (2005).

[37] G. Höhler et al., Nucl. Phys. **B114**, 505 (1976).

[38] R. B. Wiringa, V. G. J. Stoks, and R. Schiavilla, Phys. Rev. **C51**, 38 (1995).

[39] S. Galster et al., Nucl. Phys. **B32**, 221 (1971).

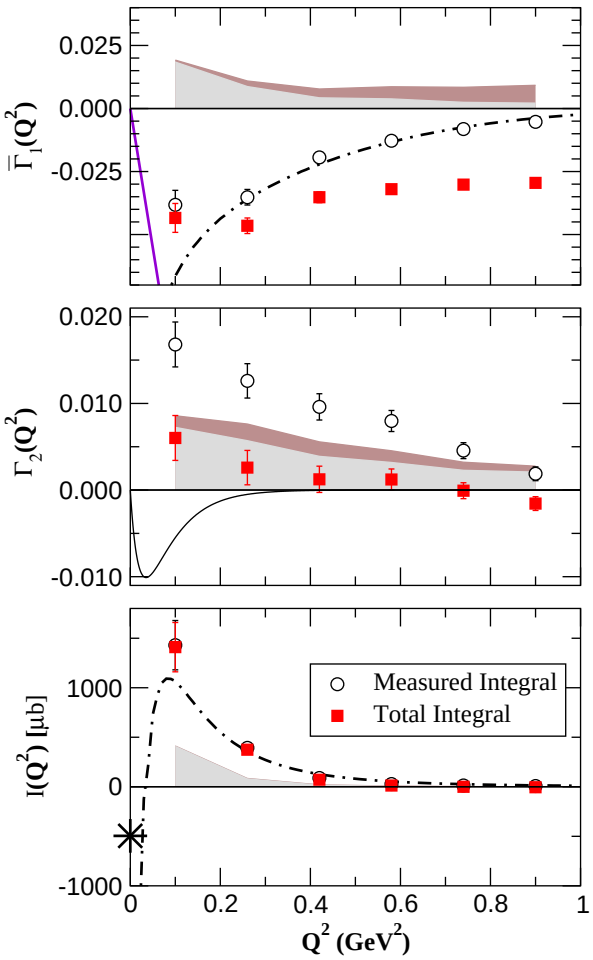

FIG. 1: ^{3}He spin-structure moments. **Top** : $\overline{\Gamma}_1(Q^2)$ compared to the PWIA model described in text (dot-dash), and the GDH sum rule slope (solid). **Middle** : $\Gamma_2(Q^2)$ along with the elastic contribution [21] (solid) to the moment. **Bottom** : $I(Q^2)$ with $K = \nu$, compared to the PWIA model.

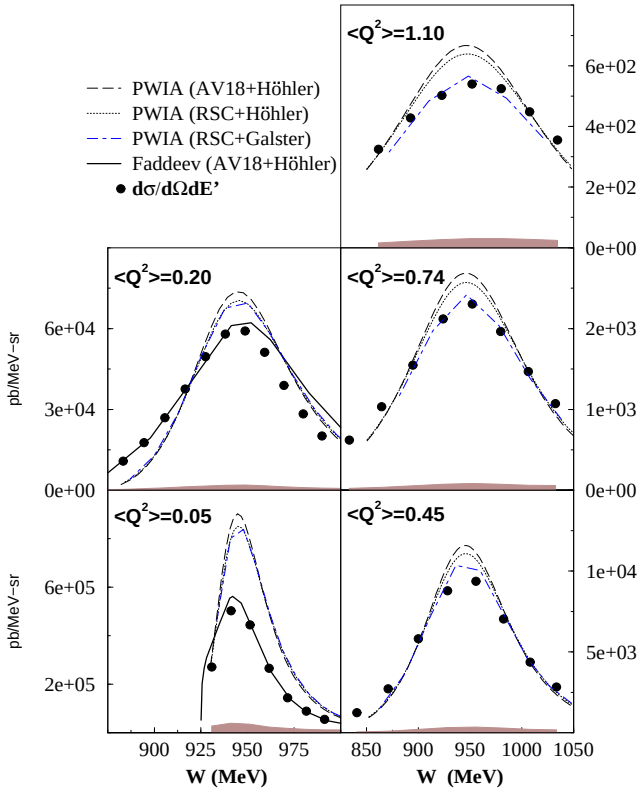

FIG. 2: ^{3}He unpolarized cross sections in the QE region compared to PWIA [24, 25] with AV18 (dashed) or RSC (dotted,dot-dashed) potential and to the Faddeev calculation [36] (solid). The error bars (bands) represent statistical (systematic) uncertainties. $\langle Q^2 \rangle$ in GeV^2.

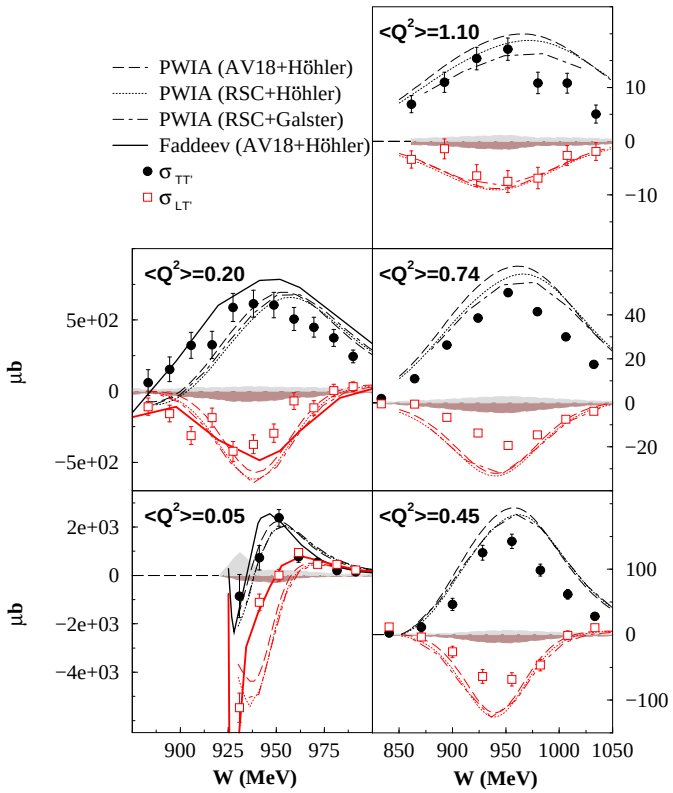

FIG. 3: Color online. ^{3}He polarized cross sections in the QE region. Curves and notations are the same as in Fig. 2.